A NEW UPPER LIMB EXOSKELETON FOR HUMAN INTERACTION WITH VIRTUAL ENVIRONMENTS AND REHABILITATION TASKS

Dimitar CHAKAROV[*], Ivanka VENEVA[**], Mihail TSVEOV[***]

[*]Institute of Mechanics, Bulgarian Academy of Sciences, Acad. G. Bonchev Str., bl. 4, 1113, Sofia, Bulgaria
[**] Institute of Mechanics, Bulgarian Academy of Sciences, Acad. G. Bonchev Str., bl. 4, 1113, Sofia, Bulgaria
[***] Institute of Mechanics, Bulgarian Academy of Sciences, Acad. G. Bonchev Str., bl. 4, 1113, Sofia, Bulgaria

mit@imbm.bas.bg, veneva@imbm.bas.bg, mtsveov@abv.bg

Abstract: In this paper the development of a new exoskeleton for the upper limb is presented. The device is designed for application where both motion tracking and force feedback are required, such as human interaction with virtual environment or rehabilitation tasks. A scheme of the mechanical structure is presented as kinematical equivalent to the structure of the human arm. Actuation of the system is based on braided pneumatic muscle. An antagonistic drive system with pulley and Bowden cable transmissions is used for each joint. A mechanical model and a software application are built. Kinematic and dynamic simulations are performed for the exoskeleton system. A control algorithm, which allows the use of two alternative control strategies for the execution of robot-in-charge and patient-in-charge execises is presented.

Key words: exoskeleton, human, upper limb, pneumatic muscle, mechanical model, simulations, control algorithm.

1. INTRODUCTION

An exoskeleton is wearable robotic device with joints and limbs corresponding to those in the human body. The exoskeleton transmits torques to human joints by actuators and has four basic functions according to the control algorithms (Perry J., Rosen J, Burns S., 2007): a) rehabilitation – fit closely to body, fulfils tasks of physical therapy in an active or passive working mode; b) Haptic device – the subject physically interacts with virtual objects, as the interaction forces are applied by the exoskeleton actuators; c) Master device – for tele-communication robot control „master-slave" as the interaction forces are applied to the slave exoskeleton from moving the master; d) Assistive device - human body amplifier, operator feels lighter the loadings, accepted by the exoskeleton.

The first modern exoskeleton arm was designed by PERCRO (Perceptual Robotics Laboratory) for replication of sensations of contacts and collisions (Bergamasco M. et al., 1994). This is a seven degree of freedom (7-DoF) ungrounded device, attached to operator's shoulder and torso. The operator holds onto the device with his/her palm. Hence, the device can only exert forces at the palm of the user. It uses DC motors with a cable transmissions. The authors of PERCRO have developed another arm exoskeletons for haptic interaction with virtual environments L-Exos (Frisoli A. et al., 2005, Frisoli A. et al., 2009). This is a five-DoF exoskeleton with a wearable structure and anthropomorphic workspace that can cover the full range of motion of a human arm. A 9-DoF under-actuated exoskeleton arm using pneumatic actuators is developed by (Lee,S. et al., 1998). Their device allows full reproduction of the human arm's workspace by the exoskeleton. An alternate arm exoskeleton developed at the Korea Institute of Science and Technology addresses the limited wearability issues of previous designs by using parallel mechanisms and pneumatic actuators (Jeong Y. et al., 2001). The wearable Salford arm addresses some of the issues and limitations of earlier designs (Tsagarakis N.G., Caldwell Dg. 2003, Tsagarakis, N.G., Tsachouridis, V., 2003). For example, nearly ninety percent of the human arm's workspace can be replicated with their device. Pneumatic muscle actuators (PMA) were selected due to their high power-to-weight ratio. Soft arm–exoskeleton was used in physiotherapy and training. The design of a seven-DoF powered cable-driven arm exoskeleton for neuro-rehabilitation is presented in (Perry J., Rosen J, Burns S., 2007). Proximal placement of motors, distal placement of pulley reductions, and open mechanical human–machine interface are few features that add performance and ease-of-use of the device. Additional characteristics include low inertias, high-stiffness links, and backdrivable transmissions without backlash. The design achieves full-workspace ranges of motion.

The objective of the work presented in this paper is to create a new concept of an upper-limb force-feedback exoskeleton with a wearable structure and anthropomorphic workspace that can cover the full range of motion of a human arm. Device can be used for application where both motion tracking and force feedback are required, such as human interaction with virtual environments or rehabilitation tasks.

2. MECHANICAL STRUCTURE AND ACTUATION SYSTEM

The exoskeleton mechanical structure is designed to fulfil the following requirements for wearable devices: light with low mass/inertia; safety; comfort; anthropomorphic workspace arm, extensive range of motion, etc. (Tsagarakis N.G., Caldwell Dg. 2003).

Usually the mechanical arm structure has 5 DoF corresponding to the natural motion of the human arm from the shoulder to the elbow, but excluding the wrist and the hand. The

human arm has 3 DoF in the shoulder (flexion/extension, abduction-adduction and lateral-medial rotation) and 2 DoF at the elbow (flexion/extension and pronation-supination of the forearm), Fig. 1.

The device usually is build up of a serial kinematic structure with rotational joints equivalent to the structure of the human arm (Bergamasco M. et al., 1994). A closed loop chain structure is build up when the human arm is linked to the exoskeleton, Fig. 1.

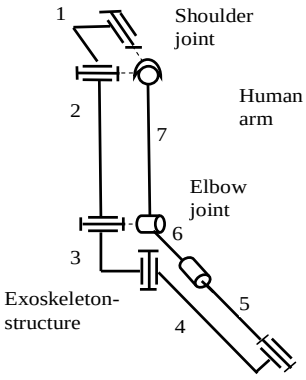

Fig. 1. Exoskeleton structure, and a human arm

The first two rotation joints are mutually orthogonal crossing the human shoulder with the same centre of rotation (Fig. 1). The third and the fourth rotational joints in the proposed structure are mutually orthogonal crossing the centre of rotation of the elbow. The fifth joint was assumed to be coincident with the forearm, in order to allow the prono- supination of the wrist. This joint is non-actuated. The closed loop kinematics structure including human and exoskeleton structures has n = 7 movable links, p_5 = 7 rotation joints with 1 d.o.f., and p_3=1 spherical joint with 3 d.o.f. According the equation $h = 6n - 5p_5 - 3p_3$ it possesses *h* =*4* d.o.f.

The presented structure meets the requirements of a powered exoskeleton in which two equal type universal joints are used, one is placed in the shoulder and one in the elbow. In this structure, the movement of the four rotation joints is equivalent of the human arm movement. The exoskeleton structure is constructed primarily from aluminium and composite materials, with high stress steel joint sections. The total weight of the uncompensated orthosis should be less than 2 kg.

The actuation system should have the following advantages: excellent power/weight ratio with inherent safety, natural compliance, low cost. The above advantages are due to the use of braided pneumatic muscle actuators (PMA). These actuators provide a low cost actuation source with a high safety due to the inherent compliance. Self-made actuators with internal diameter 10 and 20 mm were used since it permits greater control over the dimensions, forces and general performance. The maximal permissible contraction *h* of the pneumatic muscles is 30% of the nominal length *Ln*.

Joint motion/torque on the exoskeleton arm is achieved by antagonistic torques through cables and pulleys driven by the pneumatic actuators. Two acting elements, A1 and A2, work together in an antagonistic scheme simulating a biceps-triceps system to provide the bidirectional motion/force, (Fig.2). Bowden cable transmissions C1 and C2 are used for the coupling between the muscles and the pulley. The pulleys are fastened on the arm segments following joint shafts. All the actuators are mounted to the immovable base 0 through force measurement loading cells S1 and S2. High precision rotation sensors S3 are mounted in the joints.

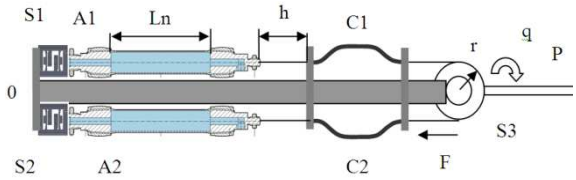

Fig. 2. Antagonistic scheme for joint motion/torque

All actuators are mounted on the exo-shell on the operator's back. The shoulder adduction/ abduction actuators are directly coupled with the shoulder pulley by steel cables, Fig. 3. The shoulder flexion extension, the elbow flexion extension and medial/lateral rotation actuators are coupled with the cables to pulleys mounted on the joints.

Fig. 3. Concept design of the exoskeleton arm

3. MECHANICAL MODEL AND SIMULATIONS

Kinematic and dynamic evaluations of the system are carried out. Mechanical model of the exoskeleton structure is build up, according to the kinematics scheme shown in Fig. 1.

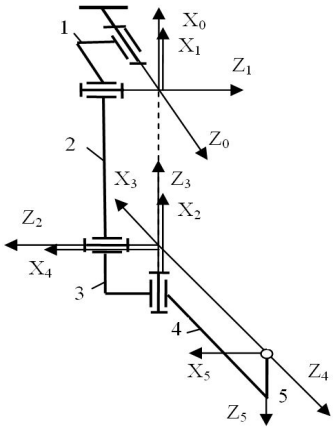

Fig. 4. Kinematics scheme with Denavit-Hartenberg reference frames

The constructed model of upper limb exoskeleton includes a serial structure with four rotating joints. Denavit-Hartenberg convention is used (Sciviacco L., B. Siciliano, 2005) for selecting reference frames as it is shown in Fig.4. The serial structure possesses h = 4 d.o.f. Independent parameters for evaluation of the system kinematics are the motion parameters in the four joints of the exoskeleton q1, q2, q3 and q4, corresponding to the four basic motions of the upper limb: Shoulder abduction/ adduction, Shoulder flexion/ extension, Elbow flexion and Shoulder med./lat. rotation.

The model includes 4 frames attached to mobile links 1,2,3 and 4, base frame attached to "immobile" link 0 and a end-effector frame 5. The four parameters describe the relation between every two consecutive coordinate frames. Denavit-Hartenberg parameters, used to describe the exoskeleton arm model, are presented in Table 1.

Tab.1. Denavit-Hartenberg parameters and mass of the links.

	q	d [m]	a [m]	α [rad]	m [kg]
Link 1	q_1	0	0	π/2	0.349
Link 2	q_2	0	0.316	π	0.411
Link 3	q_3	0	0	-π/2	0.28
Link 4	q_4	0	0	-π/2	0.509
Link 5	0	0.432	0	π/2	3.47

On the basis of the parameters in Table 1 the Denavit-Hartenberg principle gives the homogeneous transformation matrices $T_{i-1,I}$ for i= 1,…,5. After computing them

$$\mathbf{T}_{0,n} = T_{0,1} * ... * T_{n-1,n.} \tag{1}$$

we derive the position and orientation of frame n with respect to frame 0. The parameters of relative movements in the exoskeleton joints 1…h are the generalized parameters in the model:

$$\mathbf{q} = [q_1,...,q_h]^T \tag{2}$$

The coordinates and orientations of the exoskeleton end-effector are presented by the vector

$$\mathbf{X} = [X_1,...,X_\nu]^T, \nu \le 6 \tag{3}$$

The relation between the generalized parameters (1) and the coordinates of the end-effector (2) is set by the direct kinematic problem. Regarding positions and velocities, we formulate that problem introducing the following equalities:

$$\mathbf{X} = \mathbf{\Psi(q)} \tag{4}$$

$$\dot{\mathbf{X}} = \mathbf{J}\dot{\mathbf{q}} \tag{5}$$

Here

$$J = \left[\frac{\partial X}{\partial q}\right] \tag{6}$$

is the (*v x h*) matrix of Jacoby.

To solve the direct kinematics problem (4) we use the matrix equation (1). The homogeneous transformation matrix $\mathbf{T}_{0,n}$ includes the rotation matrix $\mathbf{R}_{0,n}$ of frame n with respect to frame 0 and the translation vector $\mathbf{p}_0 = [p_{0x}, p_{0y}, p_{0z}]^T$ from the frame 0 to the frame n:

$$\mathbf{T}_{0,n} = \begin{bmatrix} \mathbf{R}_{0,n} & \mathbf{p}_0 \\ 0^T & 1 \end{bmatrix} \tag{7}$$

The (3x3) rotation matrix $\mathbf{R}_{0,n}$ gives a description of the body frame orientation

$$\mathbf{R}_{0,n} = \begin{bmatrix} r_{11} & r_{12} & r_{13} \\ r_{21} & r_{22} & r_{23} \\ r_{31} & r_{32} & r_{33} \end{bmatrix} \tag{8}$$

It is characterized by nine elements which are not independent but related by six constrains (Sciviacco L., B. Siciliano, 2005). This implies that three parameters are sufficient to describe orientation of a rigid body in space. There are different approaches to describe the orientation. Some of them are known as minimal representation (for example Euler angles, XYZ angles etc. using 3 parameters), others of them are known as nominal representation (for example angle and axis or unit quaternion, using four parameters).

To describe the exoskeleton body's orientation for virtual reality realization and to avoid singularities it is adequate to apply unit quaternion defined as

$$O = \{\eta;\varepsilon\} \tag{9}$$

where η is the scalar part of the quaternion and $\boldsymbol{\varepsilon}=\{\varepsilon_x,\varepsilon_y,\varepsilon_z\}^T$ is the vector part of the quaternion. The quaternion parts corresponding to the given rotation matrix (8) can be computed by

$$\eta = 1/2\sqrt{r_{11}+r_{22}+r_{33}+1} \tag{10}$$

$$\boldsymbol{\varepsilon} = \frac{1}{2}\begin{bmatrix} \mathrm{sgn}(r_{32}-r_{23})\sqrt{r_{11}-r_{22}-r_{33}+1} \\ \mathrm{sgn}(r_{13}-r_{31})\sqrt{r_{22}-r_{33}-r_{11}+1} \\ \mathrm{sgn}(r_{21}-r_{12})\sqrt{r_{33}-r_{11}-r_{22}+1} \end{bmatrix} \tag{11}$$

Here the following restrictions exist:

$\eta \ge 0$, $\eta^2+\varepsilon_x^2+\varepsilon_y^2+\varepsilon_z^2=1$

Equation (5) express the linear velocity $\dot{\mathbf{p}}$ and angular velocity **w**, as a function of the joint velocity $\dot{\mathbf{q}}$. It can be presented as two matrix equations:

$$[\dot{\mathbf{p}}] = [\mathbf{J_p}]\dot{\mathbf{q}} \tag{12}$$

$$[\mathbf{w}] = [\mathbf{J}_0]\dot{\mathbf{q}} \tag{13}$$

Above $\mathbf{J}_p$ is the (3 x h) matrix relative to the contribution of the joint velocities $\dot{\mathbf{q}}$ to the end – effector linear velocity $\dot{\mathbf{p}}$, while $\mathbf{J}_0$ is the (3 x h) matrix relative to the contribution on the joint velocities $\dot{\mathbf{q}}$ to the end-effector angular velocity **w**.

The link between the effective generalized torques (14) and the external forces (15) applied at the end effector can be defined (16) corresponding to (12) and according to the principle of virtual work

$$\mathbf{Q} = [Q_1,...,Q_h]^T \tag{14}$$

$$\mathbf{P} = [P_x,P_y,P_z]^T \tag{15}$$

$$\mathbf{Q} = \mathbf{J_P}^{\mathbf{T}}\mathbf{P} \tag{16}$$

Above $\mathbf{J}_p^T$ is (h x 3) transpose of the Jacobian matrix of equation (12).

In virtual reality tasks, the vector of the external forces (15) represents the desired force on the end effector, when user's movements correspond to contact with a virtual surface. Let $\mathbf{dX= X_{ref}-X}$ is the virtual deviation of referent position. Cartesian stiffness matrix **K** gives the relation between desired forces on the end effector and Cartesian coordinates of the end effector.

$$\mathbf{P} = \mathbf{KdX} \tag{17}$$

In linear case when **P** and d**X** are (3 x 1) matrices, stiffness matrix **K** is a symmetric (3 x 3) matrix. It is a positive, semi-definite matrix. Appropriate values of the stiffness matrix elements define a desired magnitude and direction of the end effector force in virtual deviation of referent position.

The gravity of exoskeleton links and the gravity of human arm influences on the behavior of the end-effector. The potential energy stored in the exoskeleton arm is given by the sum of the contribution relative to each exoskeleton link:

$$U = \sum_{i=1}^{n} m_i \mathbf{g}_o^T \boldsymbol{\rho}_i \quad , \; i = 1,\ldots,5 \tag{18}$$

where m_i is the mass of link i, $\mathbf{g}_0=[g_x,g_y,g_z]^T$ is the gravity acceleration vector in the base frame and $\boldsymbol{\rho}_i =[\ \rho_x,\ \rho_y,\ \rho_z]^T$ is position vector of the i-th link centre of mass in the base frame. The vector of gravity moments generated at joints of the exoskeleton arm is

$$\mathbf{Q_g} = [Q_{g1},\ldots,Q_{gh}]^T , \tag{19}$$

Components of the gravity vector (19) can be found after differentiation of (18) with respect to generalized parameters (2)

$$Q_{gj} = \sum_{i=1}^{n} m_i \mathbf{g}_o^T \frac{\partial \boldsymbol{\rho}_i}{\partial q_j} , \qquad j = 1,\ldots, h \tag{20}$$

The gravity moments are configuration-dependent because the centers of mass vectors are dependent on join positions:

$$Q_{gj} = \sum_{i=1}^{n} m_i \mathbf{g}_o^T \mathbf{J}_{p_i}(q_j) , \qquad j = 1,\ldots, h \tag{21}$$

Generalized torques in the joints as a result of links gravity and external forces applied at the end effector (16) are given by the following equation

$$\mathbf{Q} = \mathbf{J}_p^T\mathbf{P} + \mathbf{Q}_g \tag{22}$$

4. SIMULATONS

Using the built model, MATLAB simulations are conducted. The mass and geometric parameters are defined. The segments length of the upper limb is dependent on the height of individual (Pons, J.L. 2008). The exoskeleton will be constructed for usage by an average adult, height of H=1.70 m. For a human possessing height of H=1.70 m, the following values of the elements of the upper limb are derived and for the positions of their mass centers, shown in Table 2. The limb segments' masses are derived according to the weight of the individual (Tözerem, A. 2000). The following values for the weights of the upper limb elements are derived for an individual with weight M=70 kg and are shown in Table 2. The total mass of the upper arm is estimated as 3.47 kg.

Tab.2. Length and mass of the human arm segments corresponding to an individual having height H=1.70 [m] and body mass M=70 [kg].

	Length [m]		**Mass [kg]**	
Upper arm	L1=0.186H	L1=0.316	M1=0.027M	M1=1.89
Proximal Centre of Mass	C1=0.436L1	C1=0.138		
Forearm	L2=0.146H	L2=0.248	M2=0.016M	M2=1.12
Proximal Centre of Mass	C2=0.43L2	C2=0.107		
Hand	L3=0.108H	L3=0.184	M3=0.006M	M3=0.46
Proximal Centre of Mass	C3=0.506L3	C3=0.093		

Geometric parameters of the exoskeleton in Table 1 are same as the human upper limb parameters. The exoskeleton elements are made of aluminium, the mass of the elements are estimated and shown in Table 1. The entire weight of the exoskeleton is 1.549 kg, without some additional elements such as shells, soft connections, and others. In the Table 1 the human arm mass is given as mass on the end effector m_5. Input data for simulations are the motion parameters (2) in the four joints of the exoskeleton q_1, q_2, q_3 and q_4. It has been set a simultaneous change of the parameters within the ranges: q_1 (-90;0), q_2(0;-90), q_3(0;-90), q_4 (0; 90). Resulting motion of the arm is presented on Fig.5.

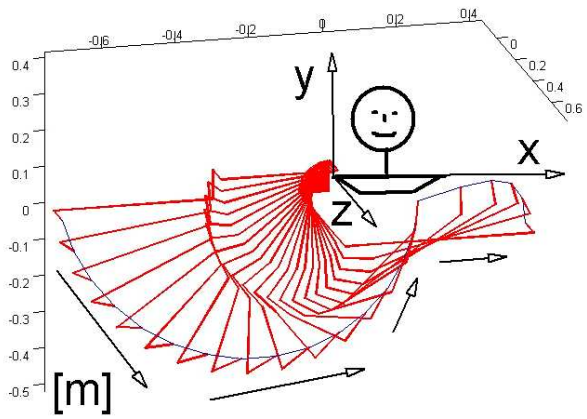

Fig.5. Motion of the exoskeleton arm

As a result of the simulations, the exoskeleton joint torques Q_{g1}, Q_{g2}, Q_{g3} and Q_{g4} (21) deviation is derived, corresponding to the change of the input angles q_1, q_2, q_3 and q_4. The torques are evaluated when the system is loaded by exoskeleton masses and also of the human arm, concentrated on the end effector. The torque variation while moving is shown in Fig. 6a). In the next experiment, in the final position of the exoskeleton arm, an external force $|\mathbf{P}|$ = 10 N is applied

(15). It is set P_x= 0 and sinusoidal variation of the components P_y,P_z , as **P** rotates in yz plane. The torque change as a result of links gravity and external forces variation (22) is shown in Fig.6b).

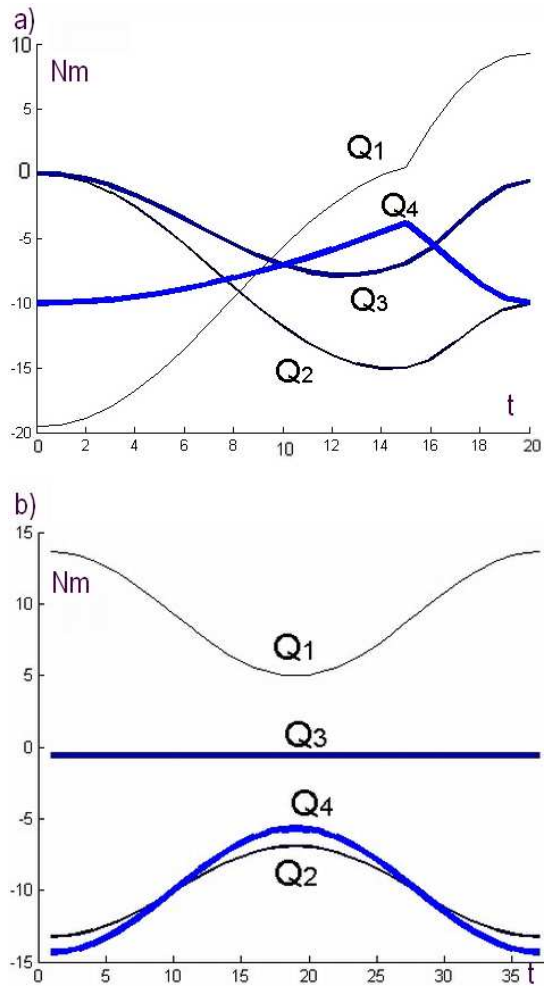

Fig. 6. Joint torque variation: a) as a result of arm motion; b) as a result of an external turning force.

Additional simulations are conducted using software package SOLID DYNAMICS'04. Model of the mechanical system upper limb - exoskeleton is build up according to the kinematics scheme shown in Fig. 1. The same geometric parameters are used, shown in Table1 and Table2. Bodies are modelled with simple geometric figures- cylinder or rectangle possessing the same mass parameters, shown in Table1 and Table2. It has been set as in the previous experiment a simultaneous change of the parameters in the four joints of the exoskeleton q1, q2, q3 and q4, expressed as the movement shown in Fig.5.

As a result of the carried out simulations, the exoskeleton joint torques deviation is derived Q1, Q2, Q3 and Q4, corresponding to the input coordinates q1, q2, q1 and q4. The torques are evaluated for three cases: a) when the system is loaded only by exoskeleton masses; b) masses of the exoskeleton are estimated and those of the arm: c) except masses of the exoskeleton and those of the arm, the loading of the end effector of 1 kg is assessed, additionally. The torque variation for the three cases are shown in Fig. 7 a), b) and c) and the deviation boundaries for the cited above three cases is presented in Table 3.

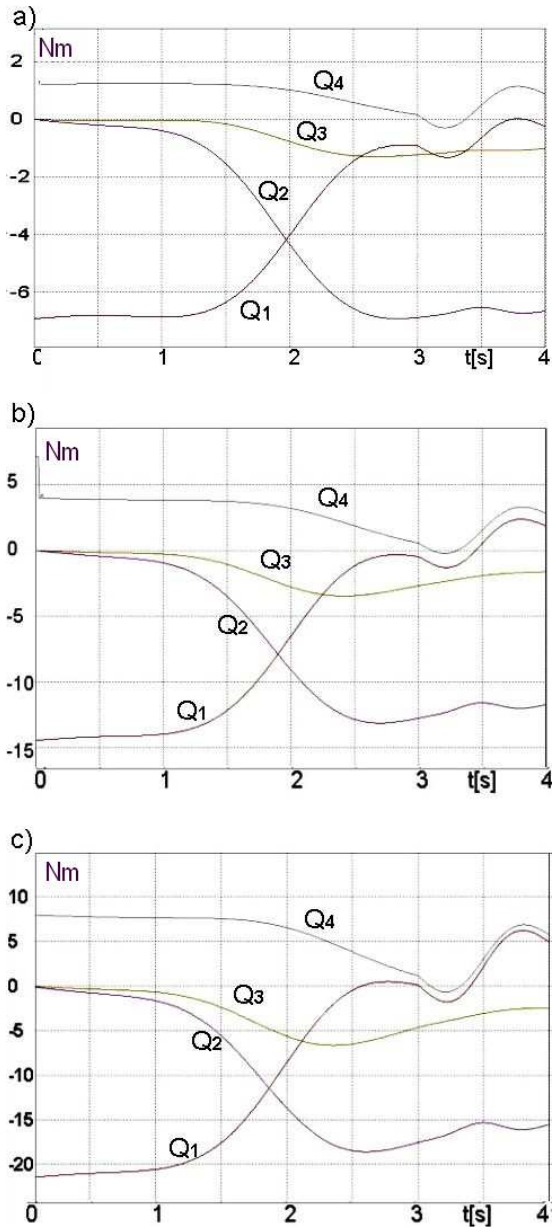

Fig.7. Joint torques variation for the three cases: a)when the system is loaded only by exoskeleton masses; b)masses of the exoskeleton are estimated and those of the arm: c) a load of 1 kg was added at the end-efektor besides of the other masses.

Tab.3. Deviation boundaries of the exoskeleton joint torques.

	a) [Nm]	**b) [Nm]**	**c) [Nm]**
Shoulder abduction/ adduction- Q1	-6.9 ; 0	-14.2 ; 2.2	-21.1 ; 6.1
Shoulder flexion/extension– Q2	0 ; -6.8	0 ; -13.1	0 ; -18.4
Elbow flexion – Q3	0 ; -1.3	0 ; -3.2	0 ; -6.8
Shoulder med.rotation/ lat.rotation-Q4	1.2 ; -0.2	2.8 ; -0.1	7.6 ; -0.4

According to the performed assessment and results shown in Fig.6 and Fig.7, the built up exoskeleton can be designed in order to ensure torque control at unidirectional joint loading for Shoulder joint to the values $|Q_{sh}|$ =22 Nm, and for Elbow joint to the values $|Q_{el}|$= 8.0 Nm. The necessary force of each muscle, by pulley radius r = 0.0315 m can be calculated for Shoulder joint F_{sh} = 698 Nm, and for the elbow joint F_{el} = 254 Nm. At antagonistic action of

both muscles, the same force value should be reached by the muscle antagonist in order to keep up a constant position in the joint at variation or zeroing of the loading.

The different load in each joint changes the range of the joint motion. In the shoulder joint with ø20 mm PMA, when the load is Q_{sh} = 22 Nm the muscle contraction can be assumed to reach 15% of the nominal length Ln. In a lower load the possible contraction of the muscles increases. The load effected only by the exoskeleton weight (Q_{sh} = 6.9 Nm), can achieve muscle contraction of 24%. Such a way, when in the first case the range of join motion is 90^0, in the second case it is 144^0.

At the elbow joint with the ø10 mm PMA, the joint range of motion changes to the same values.

5. CONTROL SCHEME

Open loop impedance control (Craig R. at al. 2000) will be used for the overall exoskeleton system (Fig. 7). This scheme will allow the use of two alternative control strategies for the execution of robot-in-charge and patient-in-charge exercises.

In a robot-in-charge task, the exoskeleton moves the human arm by displacing the equilibrium position X_{ref}-X along a desired trajectory, using an relatively high impedance K. In a patient-in-charge task, the patient initiate the virtual task and the control should be able to provide the patient with an assistive torque with a near-zero output impedance K.

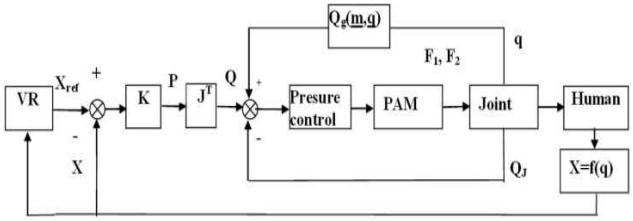

Fig.7. Control scheme

Joint torque control has been implemented on each joint. Using the torque feedback from the torque sensors on each actuator, a high bandwidth torque control loop can be formed around each individual joint. The joint torque $Q_J = r\,(F_1 - F_2)$ is a function of measured actuator forces F_1 and F_2 and pulley radius r. A gravity compensation term is included in the scheme too.

6. CONCLUSIONS AND FUTURE WORK

In this work, the development of a new exoskeleton of the upper limb is presented. The choice of a mechanical structure is shown equivalent to the structure of the human arm. A drive system is selected based on braided pneumatic muscle actuators and antagonistic drive scheme for each joint is shown using pulley and Bowden cable transmissions.

A mechanical model is built, where kinematics and dynamic parameters are evaluated. Kinematic and dynamic simulations are performed based on the mechanical model. A control algorithm is presented, which allows the use of two alternative control strategies for the execution of robot-in-charge and patient-in-charge exercises.

As a future work, the performed kinematic and dynamic evaluations must be refined after design adjustment of all the details, the final force characteristics and the motion must be derived , and the control software to be optimised.

REFERENCES

1. **Perry J., Rosen J, Burns S.** (2007). Upper-limb powered exoskeleton design. *IEEE/ASME Transactions on Mechatronics,*. Vol.12, No4, August 2007, pp.408–417.
2. **Bergamasco M., B. Allotta, L. Bosio, L. Ferretti, G. Perrini, G. M. Prisco, F. Salsedo, And G. Sartini**, (1994). An Arm Exoskeleton System for Teleoperation and Virtual Environment Applications, *IEEE Int'l Conf. Robot. Automat.*, vol. 2, 1449–1454.
3. **Frisoli A., Rocchi F, Marcheschi S, Dettori A, Salsedo F, Bergamasco M.,** (2005). A new force-feedback arm exoskeleton for haptic interaction in virtual environments. *WHC 2005. First Joint Eurohaptics Conference and Symposium on Haptic Inter-faces for Virtual Environment and Teleoperator Systems* , p.195–201.
4. **Frisoli A., Fabio Salsedo, Massimo Bergamasco, Bruno Rossi And Maria C. Carboncini**, (2009). A force-feedback exoskeleton for upper-limb rehabilitation in virtual reality, *Applied Bionics and Biomechanics,* Vol. 6, No. 2, June 2009, 115–126.
5. **Lee,S., S. Park, M. Kim, And C.-W. Lee,** (1998). Design of a Force Reflecting Master Arm and Master Hand using Pneumatic Actuators. *IEEE Conference on Robotics and Automation,* May 1998, 2574–2579.
6. **Jeong Y., Y. Lee, K. Kim, Y. Hong, And J. Park**, (2001). A 7 DOF Wearable Robotic Arm using Pneumatic Actuators," *in Proceedings of the 32nd ISR International Symposium on Robotics,* April 2001, 388-393.
7. **Tsagarakis N.G., Caldwell Dg**. (2003). Development and control of a "soft-actuated" exoskeleton for use in physiotherapy and training. *Autonomous Robots.* 15(1):21–33
8. **Tsagarakis, N.G., Tsachouridis, V., Caldwell, D.G**., (2003), 'Modeling and control of a pneumatic muscle actuated joint using on/off solenoid valves', in Proceedings of the IEEE International Conference on Advanced Robotics, pp.929–934.
9. **Sciviacco L., B. Siciliano,** (2005), Modelling and Control of Robot Manipulators, Second Edition. Springer – Verlag London, ISBN 1-85233- 221- 2.
10. **Pons, J.L.** (2008). *Wearable Robots : Biomechatronic Exokeletons,* John Willey & Sons, Ltd, ISBN, 978-0-470-5194-4, England.
11. **Tözerem, A.** (2000). *Human Body Dynamics : Classical Mechanis and Human Movements,* Springer Verlag Berlin Heidelberg. Germany
12. **Craig R. Carignan, Kevin R. Cleary**,(2000) Closed-Loop Force Control For Haptic Simulation Of Virtual Environments, Haptics-e, Vol. 1, No. 2, http://www.haptics-e.org, pp1-14.

Acknowledgements: (This work was funded by the European Commission through FP7 Integrated Project VERE - No. FP7 -257695 to which the authors would like to express their deepest gratitude).